International Immunopharmacology 77 (2019) 105959

Contents lists available at ScienceDirect

International Immunopharmacology

journal homepage: www.elsevier.com/locate/intimp

Key role of organic cation transporter 2 for the nephrotoxicity effect of triptolide in rheumatoid arthritis

Qingqing Shen[a,b,1], Jingjing Wang[a,c,1], Ziqiao Yuan[a,b,c], Zhenzhou Jiang[a,b,c], Ting Shu[a,c], Dengqiu Xu[b,c], Jinyong He[a,b], Luyong Zhang[a,d], Xin Huang[a,b,c,*]

[a] Jiangsu Key Laboratory of Drug Screening, China Pharmaceutical University, Nanjing 210009, PR China
[b] Jiangsu Center for Pharmacodynamics Research and Evaluation, China Pharmaceutical University, Nanjing 210009, PR China
[c] Key Laboratory of Drug Quality Control and Pharmacovigilance, Ministry of Education, China Pharmaceutical University, Nanjing 210009, PR China
[d] Center for Drug Screening and Pharmacodynamics Evaluation, School of Pharmacy, Guangdong Pharmaceutical University, Guangzhou 510006, PR China

ARTICLE INFO

Keywords:
Triptolide
Rheumatoid arthritis
Nephrotoxicity
Organic cation transporter 2
TNF-α

ABSTRACT

Tripterygium wilfordii Hook. F. (TwHF), a traditional Chinese Medicine, is effective in treating rheumatoid arthritis (RA), but its severe nephrotoxicity limits its extensive application. The nephrotoxic mechanism of Triptolide (TP), the main pharmacological and toxic component of TwHF, has not been fully revealed. This study was designed to explore the nephrotoxicity of TP in the RA state and the potential molecular mechanism. A rat collagen-induced arthritis (CIA) model was constructed and administered with TP for 28 days *in vivo*. Results showed that the kidney injury induced by TP was aggravated in the CIA state, the concentration of TP in the renal cortex was higher than that of the medulla after TP administration in the CIA rats, and the expression of organic cation transporter 2 (Oct2) in kidney was up-regulated under CIA condition. Besides, rat kidney slice study demonstrated that TP was transported by Oct2 and this was confirmed by transient silencing and overexpression of OCT2 in HEK-293T cells. Furthermore, cytoinflammatory models on HK-2 and HEK-293T cell lines were constructed by exposure of TNF-α or IL-1β to further explore the TP's renal toxicity. Results suggested that TNF-α exposure aggravated TP's toxicity and up-regulated the protein expression of OCT2 in both cell lines. TNF-α treatment also increased the function of OCT2 and finally OCT2 silencing confirmed OCT2 mediated nephrotoxicity of TP in HEK-293T cells. In summary, the exposure of TNF-α in RA state induced the expression of OCT2, which transported more TP into kidney cortex, subsequently exacerbated the kidney injury.

1. Introduction

Tripterygium wilfordii Hook. F. (TwHF) is effective in treating rheumatoid arthritis (RA), but the narrow treatment window and severe liver and kidney toxicity limit its wide application in clinic [1]. According to the National Center for Adverse Drug Reaction Monitoring of China, there were 839 cases of adverse reactions caused by taking Tripterygium preparations from 2004 to September 2011 [2]. The latest statistical reports show that the incidence of adverse reactions of TwHF preparations is about 26.7–58.1% [3], of which nephrotoxicity accounts for 5.81% [4]. Tripterygium glycosides (TG), extracted from the roots of TwHF, is one of the mostly used preparations. Some patients developed adverse reactions such as oliguria, edema, hematuria, proteinuria and low back pain after taking TG, and even died of acute renal failure in severe cases [5]. Autopsy results showed degeneration and necrosis of renal tubular epithelial cells in the kidneys of the dead [6]. Triptolide (TP), the main pharmacological and toxic component of TG [3,4], caused degeneration and necrosis of renal tubular epithelial cells in rats and mice [7,8], and exposure of TP to the human renal proximal tubular epithelial cell line HK-2, human embryonic kidney epithelial cell line HKC and rat kidney cell line NRK-52E reduced cell viability and caused lactate dehydrogenase release, β-N-acetylglucosaminidase activation and apoptosis [9-12]. However, the detailed mechanism of its nephrotoxicity is still unclear.

RA is a chronic and inflammatory systemically autoimmune disease that causes erosive joint destruction or even disability and affects about 1% of the world population, mostly in women [13]. In the development of RA, pro-inflammatory cytokines such as TNF-α, IL-1β and IL-6 promote bone resorption of osteoclasts, inhibit differentiation of osteoblasts and increase muscle degradation, thus lead to joint destruction

* Corresponding author at: Key Laboratory of Drug Screening, China Pharmaceutical University, Nanjing 210009, PR China.
E-mail address: huangxin@cpu.edu.cn (X. Huang).
[1] These authors contributed equally to this work.

https://doi.org/10.1016/j.intimp.2019.105959
Received 8 July 2019; Received in revised form 23 September 2019; Accepted 1 October 2019
Available online 20 October 2019
1567-5769/

and muscle atrophy [14]. Reports revealed that inflammatory state aggravated the toxicity of certain drugs: lipopolysaccharide (LPS) increased hepatic injury induced by isoniazid in rats [15]; combination of LPS and allopurinol aggravated kidney damage of allopurinol in rats [16]; co-treatment of LPS and TP aggravated the liver damage of TP in mice [17]. However, the nephrotoxicity of TP in RA model animals hasn't been reported.

One of the basic functions of the kidney is to remove harmful substances and wastes in the body. The transporters, expressed on the membrane of the renal proximal tubular epithelial cells (PTEC), participate in tubular secretion and tubular reabsorption of some substances [18]. Organic anion transporter 1 (OAT1), organic anion transporter 3 (OAT3) and the organic cation transporter 2 (OCT2), responsible for the influx of drugs from the blood into the kidney, are the main uptake transporters on the basal membrane of human PTEC while multidrug and toxin excretion protein 1 (MATE1), organic cation/carnitine transporter 1 (OCTN1) and multi-drug resistance protein 4 (MRP4) are the main transporters at the apical side [19]. The substrates of OAT1 and OAT3 are usually small negatively charged molecules. Para aminohippuric acid (PAH) and adefovir are the classic substrates of OAT1 while penicillin G and estrone-3-sulfate are the classic substrates of OAT3. Probenecid (PRO) is their co-inhibitor [20]. Metformin (MET) and cisplatin are the classic substrates of OCT2 while cimetidine (CIM) is its inhibitor [21]. Considering the expression of renal transporters may change in disease state, leading to changes in the pharmacokinetics and toxicity of certain drugs [22,23], meanwhile pro-inflammatory cytokines regulate the expression and activity of some transporters [24-26], the change of TP's toxicity in the RA state is therefore possibly related to the abnormal expression of transporters. Besides, although TP in sandwich-cultured rat hepatocytes and Caco-2 cells was taken by P-gp [27-29], current reports failed to explain which transporter is responsible for its renal uptake, which may help to explain its nephrotoxicity.

Given these hypothesises, collagen-induced model (CIA) in rats was established to explore the change of nephrotoxicity and the disposition of TP after TP administration as well as the expression change of renal transporter in the CIA state; the transport properties of TP were explored in rat kidney slice and HEK-293T cells; cellular inflammatory models based on the pro-inflammatory cytokines were constructed to investigate the cytotoxicity effects of TP in inflammation state and the effects of these cytokines on transporter's expression and function.

2. Material and methods

2.1. Reagents

Antibodies against Oct2 (A8453) and Mate1 (A14559) were purchased from ABclonal Technology (Wuhan, China). Antibodies against β-actin (sc-69879) and Oat3 (sc-293264) were purchased from Santa Cruz Biotechnology (Dallas, TX, USA). Antibodies against Oct2 (ab230629, specially for immunohistochemistry) and Octn1 (ab200641) was purchased from Abcam (Cambridge, MA, USA). Secondary antibodies goat anti-rabbit IgG (31460) and goat anti-mouse IgG (31430) were obtained from Thermo Fisher Scientific (DE, USA). Analytical standards including metformin hydrochloride, cimetidine, moroxydine hydrochloride, PAH, verapamil, PRO, TP, and finasteride were purchased from National Institutes for Food and Drug Control. All primers used were purchased from Invitrogen (Carlsbad, CA, USA). Cytokines TNF-α and IL-1β were purchased from PeproTech (Rocky Hill, NJ, USA).

2.2. Animals, collagen induced arthritis (CIA) model and TP dose regimen

All animal protocols were approved by the Institutional Animal Care and Use Committee of China Pharmaceutical University and were performed in compliance with the National Institutes of Health Guide for the Care and Use of Laboratory Animals. Specific Pathogen Free-grade, female Wistar rats (6 weeks old; 140–160 g) were purchased from Vital River Laboratory Animal Technology (Beijing, China) and was kept in standard laboratory conditions (12-h light/dark cycle, 40–70% humidity, and a constant temperature of 22–24 °C). The rats were randomly assigned to four groups (n = 10): CON, CIA, TP, and CIA + TP.

To establish a CIA model, bovine type II collagen solution (CII, 2 mg/mL, Chondrex, USA) was emulsified on ice with an equal volume of complete Freund's adjuvant (Sigma-Aldrich, MO, USA) to form a stable emulsion. Rats were immunized by intradermally injecting the emulsified mixture (200 μL/rat) at their back base of tails on day 0 followed by booster injection (300 μL/rat) of CII emulsified with Freund's incomplete adjuvant (Sigma-Aldrich) on day 7 [30]. In the CON group, equal volumes of sterilized saline were injected.

Clinical scores were used to evaluate the severity of arthritis. The scoring criteria, which was defined as the sum of the scores of four paws of each rat, was as follows: score 0, normal; 1, erythema and mild swelling confined to the midfoot (tarsals) or ankle joint; 2, erythema and mild swelling extending from the ankle to the midfoot; 3, erythema and moderate swelling extending from the ankle to the metatarsal joint; and 4, erythema and severe swelling of the ankle, foot, and digits [31]. Body weight, arthritis scores, and the volume of each hind paw (using a self-made plethysmometer) were recorded every 3 days.

TP (purity HPLC-UV ≥ 98%) was purchased from Sanling Biotech (Guilin, China). The rats were given triptolide (500 μg/kg) by daily gavage or solvent solution (0.5% CMC-Na) for 28 days from day 18. Blood and urine samples of rats were collected every 7 days. 30 min after the last dose on day 45, rats were anesthetized and bled from abdominal aorta till their kidneys became pale. Rat kidneys were then harvested and weighed immediately. One of the kidneys was dissected out along the long axis of the hilum for histopathology and the concentration determination of TP. The left part was frozen in liquid nitrogen immediately and then stored at −80 °C for later use.

2.3. Blood biochemistry, histopathology examinations and immunohistochemistry

Serum creatinine (Scr) of rats were measured by assay kit (Jiancheng, Nanjing, China). Kidney injury molecule 1 (Kim-1) in rat urine was measured by Elisa kit (BOSTER Biological Technology, Wuhan, China). Kidney and joint histopathology were performed by Servicebio (Wuhan, China). Part of the kidney and joint tissues were fixed in 4% formaldehyde for more than 24 h before paraffinembedding. The sections were fixed on glass slides, stained by hematoxylin and eosin (HE) and evaluated with BX53 microscope (Olympus, Kyoto, Japan). Immunohistochemistry (IHC) analyses of Oct2 were performed using paraffin-embedded sections by Servicebio. Paraffin sections were according to a standard protocol. Antigen recovery was carried out in citrate buffer for 2 min at 100 °C. Sections were blocked with 5% bovine serum albumin (BSA) and then incubated with Oct2 antibody overnight at 4 °C. Sections were then incubated with a biotin-labeled rabbit anti-goat antibody for 30 min at room temperature and were visualized with diaminobenzidine.

2.4. Cell culture, cytotoxicity assay, and cytokines dose regimen

HK-2 and HEK-293T cell lines were kindly provided by Stem Cell Bank, Chinese Academy of Sciences. Both were maintained in Dulbecco's modified Eagle's/F12 medium (Gibco, CA, USA) supplemented with 10% fetal bovine serum, in an atmosphere of 37 °C, 5% CO_2, and 95% relative humidity. TP was prepared in DMSO as stock solution and diluted in medium before use. Cytotoxicity assay MTT was performed to determine the dose of TP. The inhibition rate was calculated as (1-A value of TP well/A value of control well) × 100%. Cytokines TNF-α and IL-1β were prepared according to manufacturer's instructions. Inflammatory cell model was constructed by adding each

Table 1
Primer sequences used in real-time PCR.

Primers	Forward sequence (5′ → 3′)	Reverse sequence (5′ → 3′)
rKim-1	ACTCCTGCAGACTGGAATGG	CAAAGCTCAGAGAGCCCATC
rOat1	AGAGTCACAGAGCCCTGCAT	GCCCAGGCTGTAGACATAGC
rOct2	CATCGAGGATGCCGAGAA	ACAGACCGTGCAAGCTAC
rMrp4	TCTGGGTGGAAATCGGAATC	GCAGAATAACCAGAATGGCCA
rβ-actin	TATCGGCAATGAGCGGTTCC	AGCACTGTGTTGGCATAGAGG
hTimp-1	CTGTTGTTGCTGTGGCTGATA	CCGTCCACAAGCAATGAGT
hβ-actin	TCATGAAGTGTGACGTGGACATC	TGCATCCTGTCGGCAATG

Table 2
Primer sequences used in siRNA transfection.

Primers	Forward sequence (5′ → 3′)	Reverse sequence (5′ → 3′)
siRNA-1	GGAUGUUAAUUUUUCGCUUTT	AAGCGAAAAAUUAACAUCCAC
siRNA-2	CCAAGUUGCCUAUACAGUUTT	AACUGUAUAGGCAACUUGGTA
siRNA-3	GGUCAGAACUCCUCAGAUATT	UAUCUGAGGAGUUCUGACCAA
Negative control	UUCUCCGAACGUGUCACGUTT	ACGUGACACGUUCGGAGAATT

cytokine for 48 h in serum-free condition and gene expression of referent inflammation marker IL-8 was measured [24,32]. To investigate the nephrotoxicity of TP on inflammatory cell model, cytokine TNF-α or IL-1β was pretreated for 24 h and then the media was changed to co-treatment with cytokine and TP for 24 h. The gene expression of Tissue Inhibitor of Metallopeptidase-1 (Timp-1) was measured to evaluate the nephrotoxicity.

2.5. hOCT2 siRNA transfection

The three small-interfering RNAs (siRNA) sequences against OCT2 and negative control were designed by Viewsolid Biotech (Beijing, China) and synthesized by GenePharma (Shanghai, China) (Table1). HEK-293T cells were firstly seeded onto poly-L-lysine (Sigma-Aldrich)-coated 12-well plates till 60% confluency. Lipo2000 (Invitrogen) was used for the siRNA transfection according to the manufacturer's instructions. 8 h after the transfection, the transfection media without serum was replaced by normal media. 24 h after the replacement, the cells were collected for western blot or used for uptake experiments (see Table 2).

2.6. Transient overexpression of hOCT2

Plasmid pLVX-hSLC22A2-PGK-Puro and corresponding mock plasmid were constructed by Biowit Biotech (Shenzhen, China). Till 50% confluence, HEK-293T cells were exposed to lipo2000-DNA mixture in medium without serum. 8 h after transfection, the transfection media was replaced by normal media. 48 h after the replacement, the cultures were processed for western blot or uptake experiments.

2.7. Uptake experiments using rat kidney slices and HEK-293T cells

Uptake experiments using rat kidney slices were conducted according to previous reports [33]. In brief, by using ZQP-86 tissue slicer (Zhixin Co. Ltd., Shanghai, China), slices of 0.3 mm thick were prepared from male Wistar rats' kidney cortex and then put in an ice-cold oxygenated incubation buffer containing 120 mM NaCl, 16.2 mM KCl, 1 mM $CaCl_2$, 1.2 mM $MgSO_4$, and 10 mM NaH_2PO_4/Na_2HPO_4, adjusted to pH 7.4. In Na^+-free condition, NaCl was replaced with N-methyl-D-glucamine in transport buffer. Two slices were randomly selected and then preincubated in a 24-well plate with 1 mL of oxygenated incubation buffer at 37 °C for 5 min. After preincubation, the kidney slices were incubated in the buffer containing drug at 37 °C for specific time. They were then rinsed with ice-cold buffer, blotted, weighed and homogenized. The amount of drug in homogenate was measured by LC-MS/MS. Kinetic parameters were calculated by fitting the data to a modified Michaelis-Menten model combined with a linear process [34]: $v = V_{max}[S]/(K_m + [S]) + P_{dif}[S]$; where S is the substrate concentration, v is the uptake rate at a substrate concentration of S, V_{max} is the maximum uptake rate, K_m is the Michaelis constant, and P_{dif} is the non-saturable uptake clearance.

Uptake experiments using cells were performed as reported [35]. Briefly, 24 h after seeded on poly-L-lysine-coated 12-well plates to reach 90% confluency, HEK-293T cells were rinsed two times and preincubated in transport buffer (125 mM NaCl, 4.8 mM KCl, 1.2 mM KH_2PO_4, 1.2 mM $CaCl_2$, 1.2 mM $MgSO_4$, 5.6 mM D-glucose and 25 mM HEPES, pH7.4) at 37 °C for 10 min. The transport buffer was removed and replaced with fresh transport buffer containing test compounds. At the end of the incubation, the medium was aspirated, and then the cells were washed three times with 1 mL of ice-cold PBS. Every sample was dissolved in 200 μL water. Half of the sample was used to determine the accumulated concentration of test compounds and the left half was used to detect the protein concentration according to BCA assay kit (Beyotime, Shanghai, China).

2.8. LC-MS/MS analysis

The concentration of TP in rat plasma samples were quantified as described before [36]. Urine samples were performed as plasma samples. For kidney homogenate, 50 μL aliquots were collected. Metformin concentration in samples was quantified as described below. 50 μL aliquots of samples were collected and 10 μL internal standard moroxydine was added into each sample. 150 μL of acetonitrile was added for protein precipitation. Each sample was vortexed for 3 min and centrifuged for 10 min at 13,300 rpm at 4 °C. 150 μL of supernatant was collected and mixed with 200 μL of 0.05% formic acid and centrifuged again for 10 min. 5 μL of supernatant was injected into the LC-MS/MS system. The system was triple quadrupole TSQ Quantum Ultra (Thermo Scientific). Analyses were operated in ESI positive ionization mode using selective reactions monitoring: *m/z* 130.1/71.1 for metformin and *m/z* 172.1/113.1 for moroxydine. Separation of the test compounds was achieved using a 150 × 3.0 mm i.d., 3.5 μm, Agilent ZORBAX SB-C18 column. The column temperature was maintained at 35 °C. The mobile phase composition was (A) water with 2 mM ammonium formate and 0.05% formic acid and (B) methanol (85:15, v/v), and the flow rate was 0.2 mL/min. The run time was 3.65 min for each injection. The linear range of metformin in rat kidney homogenate and cell lysate are 187.5–6000 ng/mL and 20–1000 ng/mL, respectively. Quantification of PAH in rat kidney homogenate was described in supplementary file.

2.9. Real-time PCR

Total RNA was isolated from the rat kidney cortex or cells with TRIzol reagent (Vazyme Biotech, Nanjing, China). Real-time PCR measurement was performed as described previously [37]. The mRNA levels were normalized against the levels of the housekeeping gene β-actin. All primers used were listed in Table 1.

2.10. Western blot assay

Western blot was performed as described previously [17]. Total protein was obtained from cells or rat renal cortex tissues in RIPA buffer (Beyotime, Shanghai, China) containing a 1% protease inhibitor cocktail (Roche Applied Science, Basel, Switzerland). The protein samples were separated by 8% SDS-PAGE and subsequently transferred to PVDF membranes (Millipore, Bedford, MA, USA). After blocking in 5% BSA in Tris-buffered saline containing 0.1% Tween-20 for 3 h at room temperature, the membranes were incubated with primary antibodies at 4 °C overnight. Next, the membranes were incubated with horseradish-

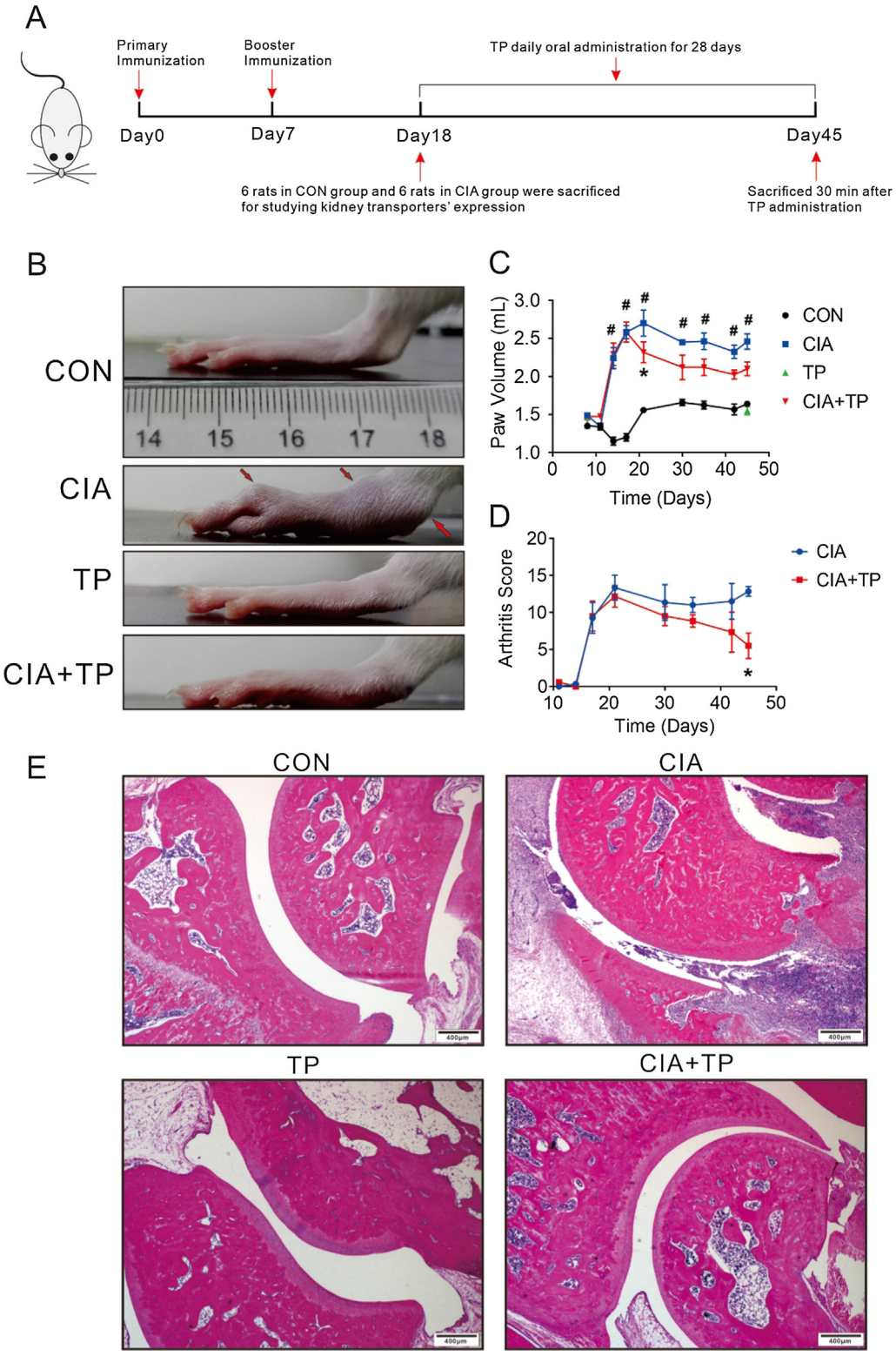

Fig. 1. TP attenuated the development of CIA in rats. (A) Sketch map of experiments *in vivo*. Appearance on day 45 (B) and volume change over time (C) of left hind paws. (D) Clinical arthritis scores over time. (E) Histopathological slices of joints (H&E staining). $^{\#}P < 0.05$ versus CON group. $^{*}P < 0.05$ versus CIA group. CIA: collagen-induced arthritis; TP: triptolide.

peroxidase-conjugated secondary antibodies at room temperature for 1 h. Protein bands were visualized and detected using the ChemiDoc Touch Imaging System (Bio-Rad Laboratories, CA, USA) and analyzed using Image J 1.42q (National Institute of Health, MD, USA).

2.11. Statistical analysis

The data were expressed as means ± SEM and the analyses were conducted by GraphPad Prism 7.0 (San Diego, CA, USA). One-way analysis of variance (ANOVA) or two-way ANOVA followed by Tukey's

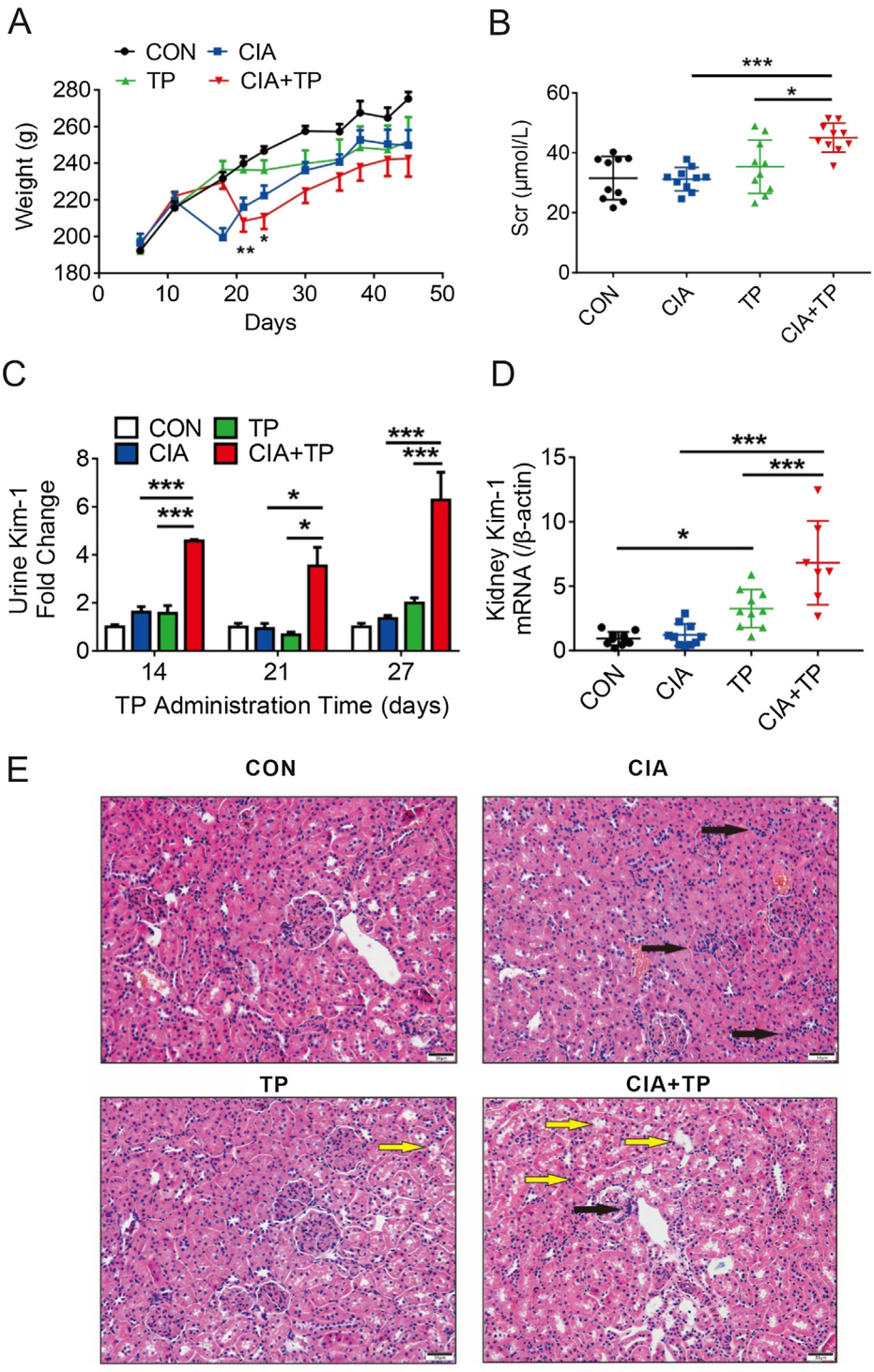

Fig. 2. CIA aggravated nephrotoxicity induced by TP in rats. (A) Body weight change over time. $^{*}P < 0.05$ and $^{**}P < 0.01$ between CIA + TP and TP groups. (B) The level of Scr on day 45. (C) Fold change of Kim-1 in rat urine after 14, 21 and 27 days of TP administration, respectively (n = 4–6). (D) The mRNA expression of Kim-1 in rat kidney cortex. (E) Histopathological slices of rat kidneys (H&E). Black arrow represents inflammatory infiltration. Yellow arrow represents shedding of epithelial cell in kidney proximal tubules of rats. In Fig. B-D, $^{*}P < 0.05$ and $^{***}P < 0.001$ between two groups. Scr: serum creatinine; Kim-1: kidney injury molecular-1. (For interpretation of the references to color in this figure legend, the reader is referred to the web version of this article.)

Multiple Comparison Test was performed to analyze the differences between groups. P values < 0.05 were considered statistically significant.

3. Results

3.1. TP attenuated the development of CIA in rats

In animal studies, CIA rats were orally administered TP (500 μg/kg) since day 18 after the primary immunization (Fig. 1A). Before the toxicity evaluation, we first assessed the CIA model and the efficacy of TP. Red and swollen metatarsi, phalanges and ankles (red[2] arrows) were found in CIA rats while 28 days of TP administration alleviated these RA symptoms (Fig. 1B) and decreased paw volume and clinical arthritis score (Fig. 1C and D). Histopathologically, the joints of CIA rats exhibited severe inflammatory infiltration, synovial hyperplasia, and bone erosion while the degree of bone destruction and inflammatory cell infiltration was markedly lower in CIA rats treated with TP (Fig. 1E). These results indicated that CIA model and the efficacy of TP were verified.

[2] For interpretation of color in Fig. 1, the reader is referred to the web version of this article.

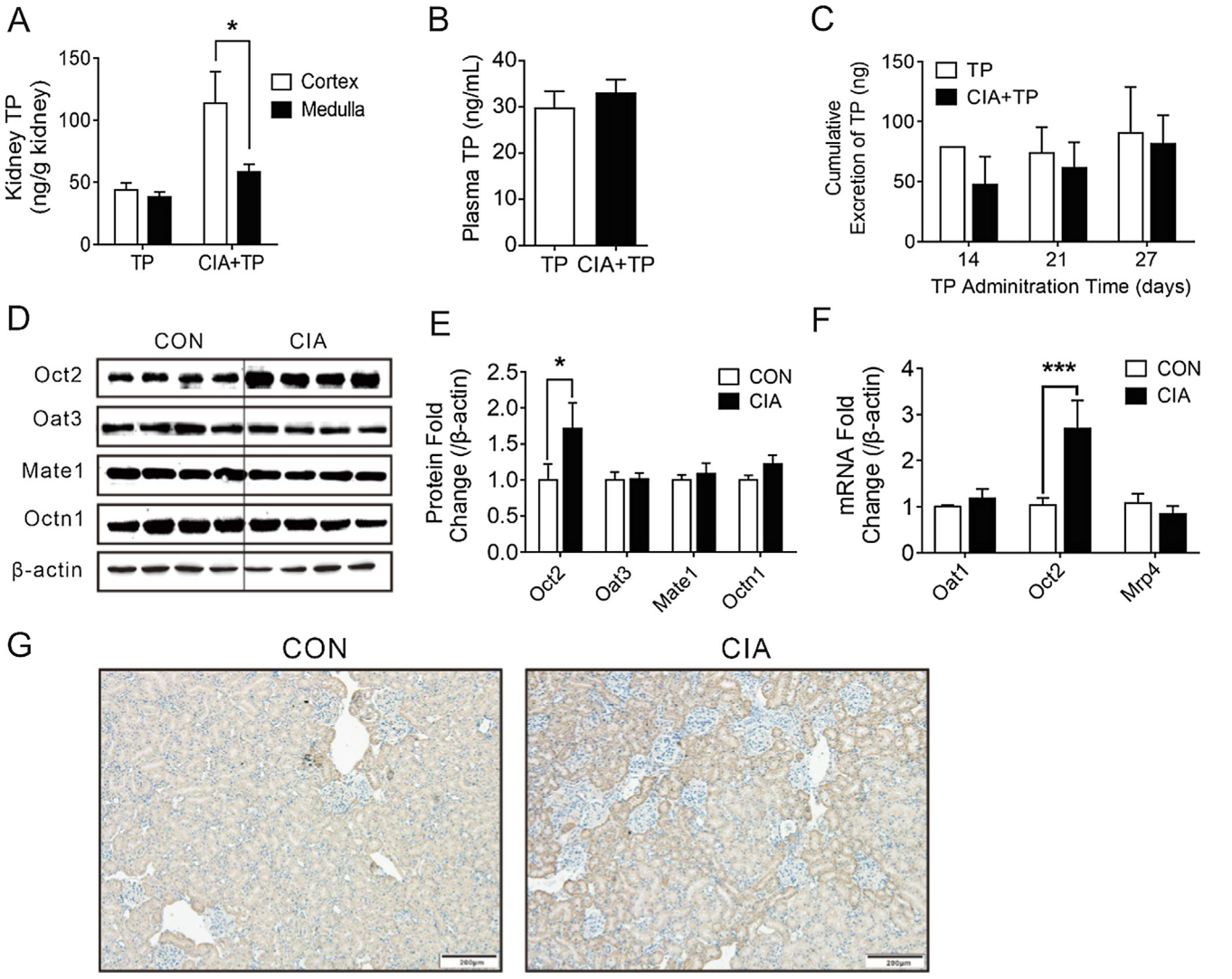

Fig. 3. CIA increased TP accumulation in rat kidney cortex and renal Oct2 expression (n = 4–6). The TP concentration levels in rat kidney (A) and plasma (B) at 30 min after the last dose of TP. (C) The cumulative excretion of TP within 3 h on day 14, 21 and 27 after TP administration. The protein (D, E) and gene expression (F) of major kidney transporters. (G) The immunohistochemistry showed the distribution of Oct2 (brown) in rat kidney. $^{*}P < 0.05$ and $^{***}P < 0.001$ between two groups. (For interpretation of the references to color in this figure legend, the reader is referred to the web version of this article.)

3.2. CIA aggravated nephrotoxicity induced by TP in rats

To investigate the nephrotoxicity difference of TP between pathological and physiological conditions, the body weight, serum creatinine, urine concentration and renal gene expression of early biomarker kidney injury molecular-1 (Kim-1), and histopathological manifestation of rat kidneys were evaluated. The body weight of the CIA + TP group was significantly lower than that of the TP group on day 3 and 6 after TP administration (Fig. 2A). The serum creatinine of the CIA + TP group rats was significantly higher than that of TP group (Fig. 2B). The urine Kim-1 levels of the CIA + TP group were significantly higher than that of the TP group 14, 21 and 27 days after TP administration (Fig. 2C). In line with this, the renal gene expression of the Kim-1 of the CIA + TP group (two extreme values 136.5 and 26.7 were culled) was about 1.8 times higher than that of the TP group and about 3.1 times higher than that of the CON group (Fig. 2D). Renal pathological slices showed that minor inflammatory infiltration was found in the CIA group (black arrow), epithelial cell shedding of kidney proximal tubule (yellow arrow) and cytoplasm loosening were found in the TP group, and major epithelial cell shedding was found in the CIA + TP group, as well as cytoplasm loosening, inflammatory infiltration and unclear lumen boundary (Fig. 2E). These results indicated that the kidney injury of the CIA + TP group was more severe than that of the TP group *in vivo*.

3.3. CIA increased TP accumulation in rat kidney cortex and renal Oct2 expression

To investigate whether the increased toxicity of TP was due to its disposition change in CIA condition, the concentration of TP in kidney, plasma and urine were measured. As shown in Fig. 3A–C, TP distributed more in kidney cortex than medulla in CIA condition, compared with TP group, but there was no difference between CIA + TP and TP group in plasma concentration and urine excretion of TP. Since drug transporters play key roles in drug disposition and excretion, the gene and protein expression levels of major kidney transporters on day 18 were detected. As shown in Fig. 3D–F, Oct2 expressed more in CIA condition, compared with control group, but no changes were found with other transporters. Immunohistochemistry results also showed that protein expression of Oct2 increased in CIA state (Fig. 3G). Oct2 also expressed more in CIA group than control group on day 45 (Fig. S1). These evidences proved that CIA condition increased TP accumulation in rat kidney cortex and renal Oct2 expression. Thus, we suspect that TP may be transported by Oct2.

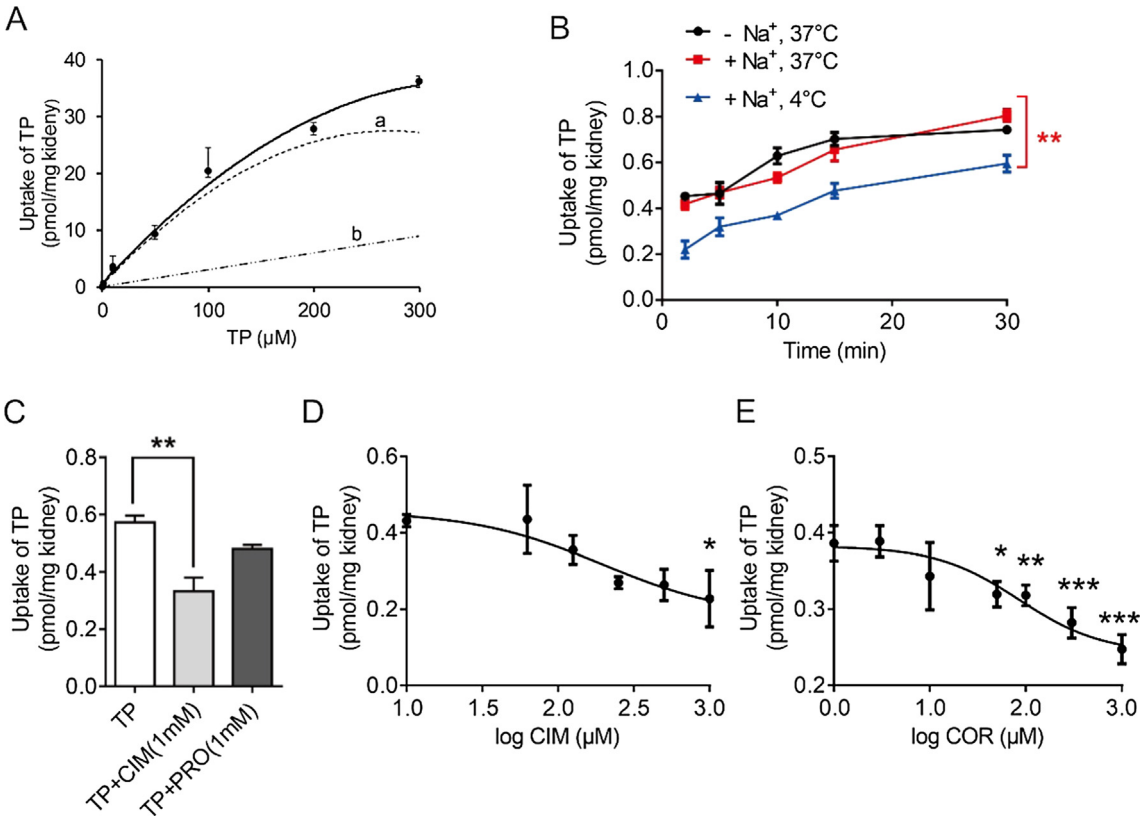

Fig. 4. TP was transported by Oct2 in rat kidney slices (n ≥ 3). (A, B) Concentration-, time-, temperature-dependence, and sodium-independence uptake of TP. CIM and COR (D, E) rather than PRO (C) inhibited the uptake of TP. CIM: cimetidine; COR: corticosterone; PRO: probenecid. The time of TP was 10 min in Fig. A. The dose of TP was 1 μM in Fig. B-E. $^{*}P < 0.05$, $^{**}P < 0.01$, and $^{***}P < 0.001$ between two groups.

3.4. TP was transported by OCT2 in rat kidney slices and HEK-293T cells

To explore whether TP was transported by Oct2, uptake experiments were performed on both rat kidney slices and HEK-293T cells. The functional activity of the rat kidney slice model was validated based on the inhibition of metformin by cimetidine. The concentration-dependent uptake of TP fitted best to the modified Michaelis-Menten model (Fig. 4A curve a) with a non-saturable process (Fig. 4A line b). The K_m, V_{max} and P_{dif} were 250.7 μM, 6.649 pmol/min/mg kidney, 0.0030 μL/min/mg kidney, respectively. In subsequent studies the dose of TP was 1 μM, which matched with rat study *in vivo* (Fig. 3A). The uptake of TP was significantly higher at 37 °C compared with 4 °C, and nearly reached saturation at 15 min (Fig. 4B). The concentration- and temperature-dependence uptake of TP suggested that transporters played roles in the renal transport of TP. Besides, the uptake of TP was sodium-independent (Fig. 4B). Since Oat1 and Oat3 (Oat1/3) relied on the maintenance of the sodium gradient [38] while Oct2 was sodium-independent [39] (Fig. S2), it was more likely that Oct2 rather than Oat1/3 played a role in renal uptake of TP. CIM and COR (Fig. 4D and E) rather than PRO (Fig. 4C) inhibited the uptake of TP, which consolidated that TP was transported by Oct2.

The time- and concentration-dependence uptake of TP were also observed in HEK-293T cells (Fig. 5A and B). To further verify whether TP was a substrate of OCT2, RNA silencing using siRNAs specific to OCT2 was applied. Different silencing efficiency of three pairs of siRNA sequences on OCT2 expression was observed after transfection, among which siRNA-2 and siRNA-3 were with high efficiency (Fig. 5C). siRNA-2 was selected for later study and TP uptake was reduced after RNA silencing (Fig. 5D). Similarly, uptake of TP was increased by transient overexpression of OCT2 (Fig. 5E and F). These results further confirmed that TP was transported by OCT2. However, it was still unclear why the expression of OCT2 was increased under CIA condition.

3.5. TNF-α aggravated nephrotoxicity induced by TP in vitro

Before the mechanism on expression change of OCT2 under CIA condition was elucidated, the nephrotoxicity difference of TP between inflammatory and normal conditions *in vitro* were investigated on HK-2 and HEK-293T cell lines. HK-2 cell inhibition rate after TP exposure for 24 h was shown in Fig. 6A, 10 nM was chosen for later toxicity tests. Since TNF-α and IL-1β were the most expressed cytokines both in the blood of rheumatoid arthritis patients and CIA rats [14,40,41], as well as potential regulators of transporters, inflammatory conditions were achieved by given these cytokines separately. Firstly, expression of the referent inflammation marker was measured after cytokine treatments in order to make sure HK-2 was fully responsive to cytokines. As shown in Fig. 6B, IL-8 mRNA expression was markedly increased after 48 h of TNF-α (8–100 ng/mL) and IL-1β (8–20 ng/mL) exposure. Accordingly, HK-2 were suitable for investigating cytokines' effects toward drug transporter expression. Subsequently, Timp-1 was used as a cytotoxicity marker. The mRNA expression of Timp-1 was not affected by cytokines alone, but was 2.9–3.4 (1.0–2.2) times more with TNF-α (IL-1β) and TP co-treatment than given TP alone at the same dose, respectively (Fig. 6C). Similar manifestations were found on HEK-293T cells (Fig. S3, 6D), but there was no toxicity difference between IL-1β and TP co-treatment and TP alone. In conclusion, TNF-α aggravated nephrotoxicity induced by TP *in vitro*. It is likely that TNF-α induced the expression or function change of OCT2.

3.6. OCT2 induced by TNF-α and led to nephrotoxicity of TP in vitro

We next explored the expression and function change of OCT2 when given TNF-α. The protein expression of OCT2 were increased in a dose-dependent manner treated with TNF-α in two cell models (Fig. 7A–D). The uptake of MET increased after the addition of TNF-α rather than IL-

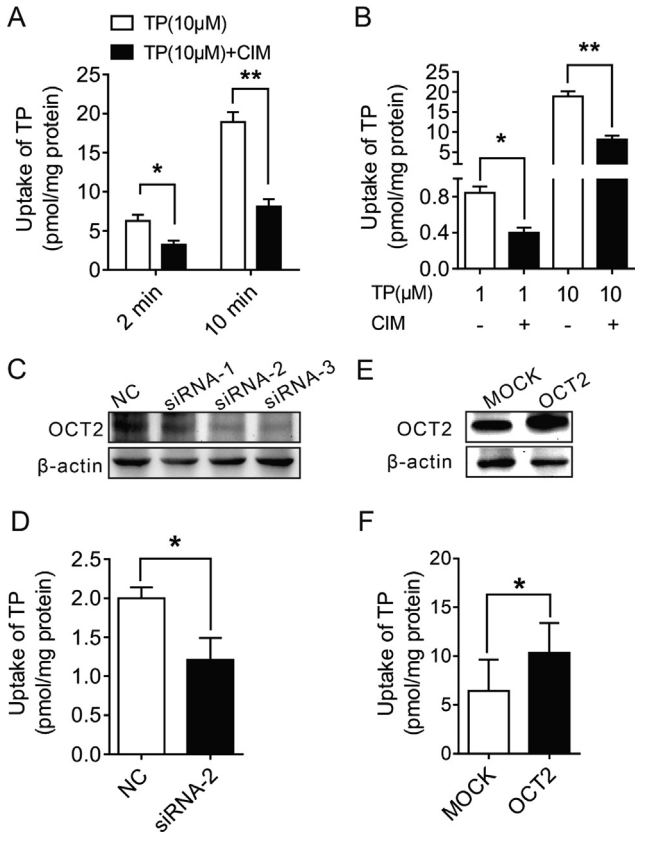

Fig. 5. TP was transported by OCT2 in HEK-293T cells (n ≥ 3). Time-(A) and concentration-(B) dependence uptake of TP. (C) Efficiency verification of siRNAs specific to OCT2 by western blot. (D) The uptake of TP by siRNA-2 transfection. (E) Efficiency verification of transient overexpression of OCT2 by western blot. (F) The uptake of TP by OCT2 overexpression. The uptake time of TP was 10 min (B, D, F) and the dose of TP was 10 μM (A, D, F). NC: negative control. $^{*}P < 0.05$ and $^{**}P < 0.01$ between two groups.

1β on HEK-293T (Fig. 7E), which showed that TNF-α might be a major player in the regulation of OCT2 expression and function. On the other hand, there was no significant toxicity after OCT2 silence when TP treatment or TNF-α and TP co-treatment on HEK-293T (Fig. 7F). These results confirmed that OCT2 was induced by TNF-α and played a key role in the nephrotoxicity of TP.

4. Discussion

This study elucidated the key role of OCT2 in the nephrotoxicity of TP in RA state. It was found that kidney injury induced by TP administration was aggravated and TP distributed more to the kidney cortex than medulla in CIA rats, and the protein expression of Oct2 was induced in the kidney cortex of CIA rats. The transport of TP was found to be mediated by OCT2 in rat kidney slices and HEK-293T cells. It was also found that TNF-α aggravated the toxicity of TP and regulated both the expression and function of OCT2 and confirmed that OCT2 mediated the nephrotoxicity of TP *in vitro*.

TG contains complex components, and its toxic reactions *in vivo* involve multiple targets. Since TP is recognized as its main pharmacological and toxic component, it was chosen as the object in this study. In previous reports, routine nephrotoxicity indexes, such as serum creatinine, urea nitrogen, kidney weight coefficient, and pathological examination showed that the nephrotoxicity of TP in rats was not obvious [9,10], which did not match with clinical reports. In this study, two solutions were proposed to solve this gap. Firstly, we suspected the renal toxicity of TP might be different under physiological and pathological conditions. Secondly, a more sensitive toxicity index was needed. Hence, a rat CIA model and a more sensitive early kidney injury biomarker Kim-1 were introduced. Consistently, the creatinine and pathological slices showed only mild toxicity after administration of TP for 28 days in rats in our study. Notably, a significant increase in urine Kim-1 (2.91 times) was observed 14 days after TP administration in CIA rats compared with CON rats treated with TP (Fig. 2C). This result suggested that the nephrotoxicity of TP was more obvious under RA condition. Urine Kim-1 may thus be used as a potential marker for clinically evaluating and predicting the risk of kidney injury in RA patients after taking TG. Timp-1, also located in PTEC, was taken as the toxicity marker *in vitro*. It was originally discovered to be a natural inhibitor of matrix metalloproteinases and involved in wound repair, regulation of angiogenesis and activation, cell proliferation, and apoptosis. Serum and urinary Timp-1 levels were reported to be associated with chronic kidney disease [42,43], and recent studies have shown that it is a potential biomarker for kidney diseases like renal ischemia-reperfusion injury [44], diabetic nephropathy [45], renal fibrosis in children with nephrotic syndrome [46], and transplanting kidney function [47]. And it was also validated as a toxic marker on HK-2 cells [48-50]. Our results showed that the gene expression level of Timp-1 was increased when co-treating TNF-α with TP than TP alone in both two cells (Fig. 6C and D), which indicated that TNF-α aggravated the toxicity of TP *in vitro*.

In animal studies, female rats were chosen. There are two reasons. Firstly, prevalence of RA is two-to-three times higher in women than men [13,51]. Also, studies showed that female Wistar rats were greatly susceptible to CIA and had low variability in clinical signs [52]. Therefore, using female rats make CIA model more stable and closer to clinic. The other reason is that previous study in our lab showed that females were more susceptible to toxicity of TP [53]. Although nearly all the kidney transporters mentioned in this paper (Oat1, Oat3, Oct2, Octn1, Mrp4 and Mate1) are more abundant in male rats than females [54], the conclusions we drew were not affected by gender. TP was transported by Oct2 rather than Oat1/3 both in male rats and females (Fig. S5).

It was known that changes in the disposition of drugs may lead to reduced efficacy and increased toxicity [55]. Therefore, we wonder whether the nephrotoxicity change of TP in RA state is due to the disposition change of TP in RA. Previous studies showed that TP metabolized rapidly in rats and the concentration of TP in rat kidney decreased 5 min after TP administration [56-58]. Considering short time interval for rats' execution and kidney harvest might cause large errors, 30 min and 1 h after the last dose of TP were chosen to measure TP's concentration, respectively. Results from 1 h after the last dose (Fig. S4), which was like Tan et al.'s report [59], might be interfered by excretion. Therefore, experiments at 30 min after the last dose was taken. It was shown that TP in CIA rats was mostly distributed in the renal cortex rather than medulla (Fig. 3A). Since the renal transporters are distributed in the renal cortex and renal cortex is the toxic site of TP, we next hypothesized that the disposition change of TP was related to the change of transporter expression in the CIA state and TP was transported by a certain transporter.

Our study first reported that the renal transport of TP was mainly mediated by OCT2 both in rat kidney slices and HEK-293T cells (Figs. 4 and 5). Although rats also express Oct1 in the proximal tubules and Oct1 may also contribute to the uptake of metformin in Fig. 5, we still hold that Oct2 is of priority. Firstly, the gene expression level of Oct2 was 2.14 ± 0.96 times high than Oct1 in rat kidney cortex (data not shown). On the other hand, since OCT1 is expressed at extremely low levels in human kidney and is mainly found in the liver, it might not be a good idea to focus on OCT1 in human kidney in transporter studies. Instead, the expression of OCT2 in human kidney is predominant [60].

Still, OCT2 stably transfected cell line is needed for further validation. Previous reports showed that the transport of TP in Caco-2 cell line and sandwich-cultured rat hepatocytes was mediated by P-gp [21,27]. It is likely that TP is imported into kidney cells by OCT2 and exported

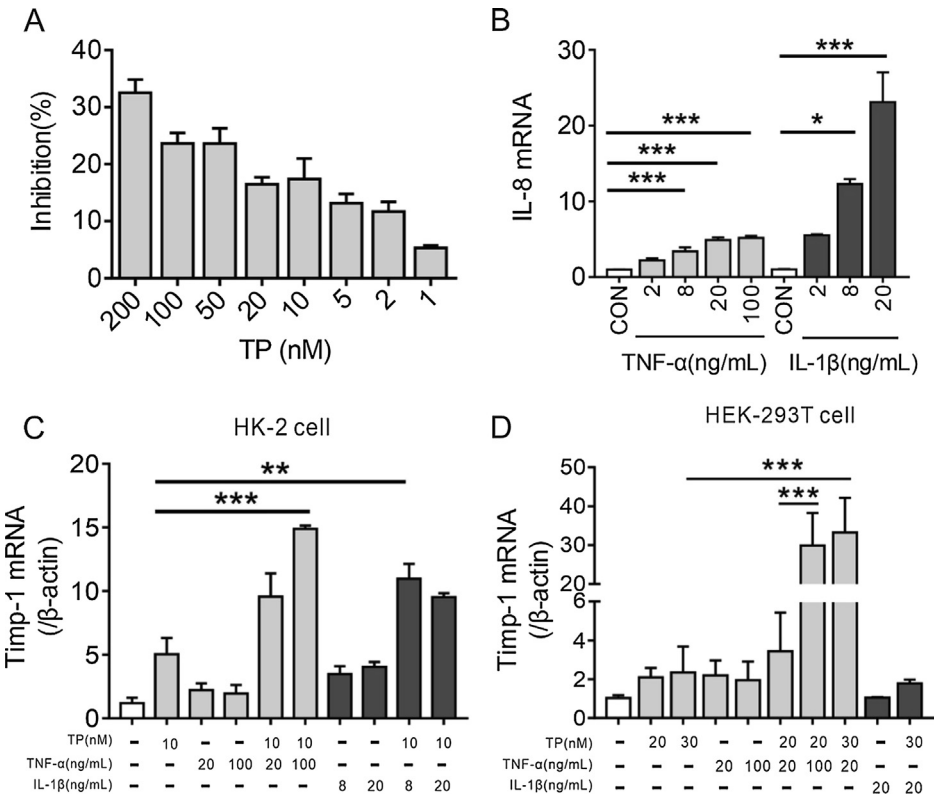

Fig. 6. Inflammatory cytokines aggravated nephrotoxicity induced by TP *in vitro* (n ≥ 3). (A) MTT results after TP treatment (1–200 nM) for 24 h on HK-2 cells. (B) Gene expression of IL-8 after administration of TNF-α and IL-1β for 48 h on HK-2. (C, D) The gene expression of toxicity index Timp-1 after administration of TP on HK-2 and HEK-293T inflammatory cell models, respectively. $^{*}P < 0.05$, $^{**}P < 0.01$, and $^{***}P < 0.001$ between two groups.

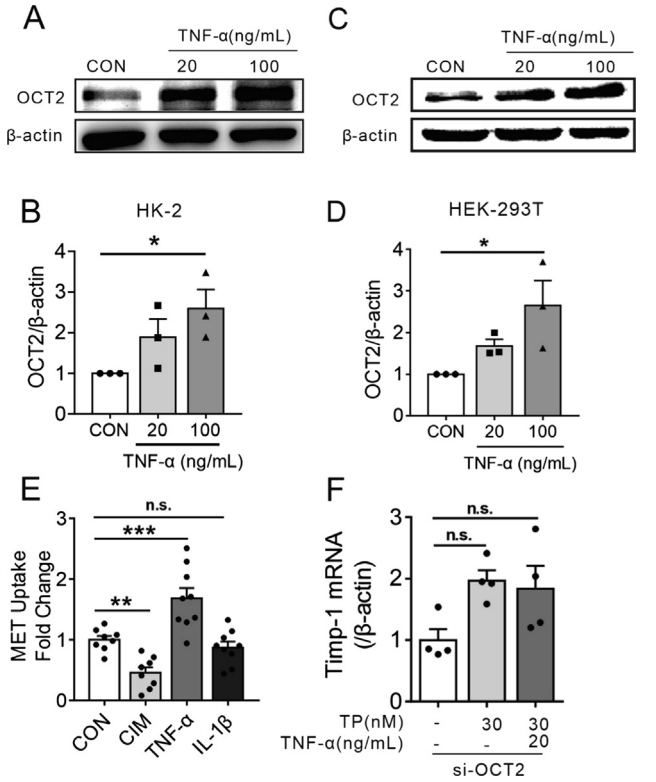

Fig. 7. OCT2 induced by TNF-α and led to nephrotoxicity of TP *in vitro* (n ≥ 3). (A, B) The expression of OCT2 after treatment with TNF-α for 48 h on HK-2 cells. (C, D) OCT2 expression after treatment with TNF-α for 48 h on HEK-293T cells. (E) The uptake of MET after TNF-α (20 ng/mL) and IL-1β (20 ng/mL) administration for 48 h; (F) The gene expression of Timp-1 when TNF-α and TP were administered after OCT2 silencing. MET: metformin; Timp-1: tissue inhibitor of metallopeptidase-1. $^{*}P < 0.05$, $^{**}P < 0.01$, $^{***}P < 0.001$ and n.s. not significant between two groups.

by P-gp into urine. Notably, transmembrane transport of certain drugs does not always rely on only one way. For example, the transport of CIM was through both passive diffusion and transport of OCT2 (dominant) [61]; the transport of berberine on kidney slices, in addition to Oct2, also mediated by passive diffusion [24]; after administration of CIM, the uptake of nitidine chloride on MDCK-OCT2 cells was still 20% left [62], indicating that there were other mechanisms besides OCT2. Our results showed that TP had considerable uptake after administration of high doses of OCT inhibitors CIM and COR in rat kidney slices (Fig. 4D and E), and only 40% of TP's transport was inhibited after OCT2 silencing in HEK-293T cells (Fig. 5E). Therefore, in addition to OCT2's transport, there may be other mechanisms involved, which remains to be studied. Since TP could cause hepatotoxicity by reducing the substrate affinity, activity, and expression at the gene and protein levels of the CYP450 isoforms [63], CYP enzymes might be involved in TP's nephrotoxicity.

This paper reports for the first time that the expression of renal transporter OCT2 was up-regulated in the CIA state (Fig. 2D–G). Since pro-inflammatory cytokines play important roles in the RA state [14], and it has been reported that cytokines regulate the expression and function of SLC family transporters [25,26,32], we suspect that inflammatory cytokines are responsible for up-regulating OCT2 expression. Lack of kidney cell model under RA, in this study, cellular inflammatory models were constructed to explore transporter's expression by directly adding TNF-α and IL-1β. Due to toxicity consistence by TNF-α exposure and inconsistence after IL-1β addition between two cell lines (Fig. 6C and D), TNF-α was considered as the main regulator of OCT2. Further verification by OCT2 knockdown *in vitro* confirmed that TNF-α up-regulated OCT2's function (Fig. 7F). Yet detailed mechanism on how TNF-α is involved in the regulation of expression and function of OCT2 remains to be studied. It may be mediated through the nuclear receptor LXR/RXR complex [64,65].

Together, we hypothesized that the increased nephrotoxicity of TP in RA state might be due to explosion of TNF-α in the blood, which up-regulated the expression of OCT2, and then transported more TP into

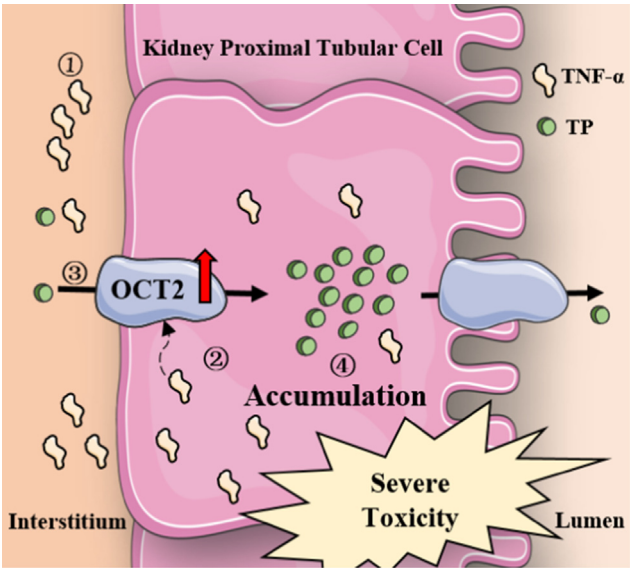

Fig. 8. Possible mechanism of nephrotoxicity of TP in the RA state. ① TNF-α erupts in the blood of RA patients. ② TNF-α up-regulates the expression of OCT2. ③ More TP was transported into the kidney by OCT2. ④ Excessive TP accumulates in the renal cortex after long-term administration, which leads to severe renal toxicity.

the kidney. After long-term administration, excessive TP accumulated in the renal cortex, which aggravated the nephrotoxicity of TP (Fig. 8). This study suggests that the toxicity of the drug may change under pathological conditions and using pathological models to evaluate the toxicity of the drug may help to fully understand the toxic mechanism of drugs, especially when the drug is a substrate for an uptake transporter. To avoid clinical kidney damage caused by TG, the substrates or inhibitors of OCT2 such as berberine and cimetidine could be used combining with TG.

Declaration of Competing Interest

The authors declare that there are no conflicts of interest.

Acknowledgements

This work was supported by the National Natural Science Foundation of China (81673684, 81703626, 81573690).

Appendix A. Supplementary material

Supplementary data to this article can be found online at https://doi.org/10.1016/j.intimp.2019.105959.

References

[1] J. Wang, N. Chen, L. Fang, Z. Feng, G.C. Li, A. Mucelli, X. Zhang, X.P. Zhou, A systematic review about the efficacy and safety of *Tripterygium wilfordii* Hook.f. preparations used for the management of rheumatoid arthritis, Evid. Based. Compl. Alternat. Med. 2018 (2018) 1567463.
[2] China Food and Drug Administration. http://samr.cfda.gov.cn/WS01/CL1989/70473.html (accessed 01 April 2012).
[3] C. Zhang, P.P. Sun, H.T. Guo, Y. Liu, J. Li, X.J. He, A.P. Lu, Safety profiles of *Tripterygium wilfordii* Hook F: a systematic review and meta-analysis, Front. Pharmacol. 7 (2016) 402.
[4] X.X. Li, F.Y. Du, H.X. Liu, J.B. Ji, J. Xing, Investigation of the active components in *Tripterygium wilfordii* leading to its acute hepatotoxicty and nephrotoxicity, J. Ethnopharmacol. 162 (2015) 238–243.
[5] Z. Huang, Q.Q. Mao, Clinical application, untoward reaction and its prevention of TWP, Drug. Eval. 2 (2) (2005) 125–128.
[6] G.Z. Huang, L. Li, L. Liu, D.M. Wei, Pathological study on autopsy died of Tripterygium intoxication——report of 4 cases, Chin. J. Integr. Trad. West. Med. 29 (2) (2009) 165–168.
[7] L. Liu, Z.Y. Wang, G.Z. Huang, Y. Liu, The influence of triptolide sub-chronic intoxication on kidney and testicle in mice, Acta Med. Universitatis. Scientiae. et Technologiae. Huazhong. 30 (3) (2001) 214–217.
[8] F. Yang, L. Zhuo, S. Ananda, T.Y. Sun, S.X. Li, L. Liu, Role of reactive oxygen species in triptolide-induced apoptosis of renal tubular cells and renal injury in rats, J. Huazhong Univ. Sci. Technolog. Med. Sci. 31 (3) (2011) 335–341.
[9] L.X. Sun, H. Li, X. Huang, T. Wang, S. Zhang, J. Yang, S. Huang, H.F. Mei, Z.Z. Jiang, L.Y. Zhang, Triptolide alters barrier function in renal proximal tubular cells in rats, Toxicol. Lett. 223 (1) (2013) 96–102.
[10] B. Shu, W.G. Duan, J.C. Yao, J.F. Huang, Z.Z. Jiang, L.Y. Zhang, Caspase 3 is involved in the apoptosis induced by triptolide in HK-2 cells, Toxicol. In Vitro. 23 (4) (2009) 598–602.
[11] Z.P. Wang, H.F. Jin, C. Li, Y. Hou, Q.B. Mei, D.M. Fan, Heat shock protein 72 protects kidney proximal tubule cells from injury induced by triptolide by means of activation of the MEK/ERK pathway, Int. J. Toxicol. 28 (3) (2009) 177–189.
[12] J. Li, J. Jin, M. Li, C.W. Guan, W.W. Wang, S.H. Zhu, Y.W. Qiu, M. Huang, Z.Y. Huang, Role of Nrf2 in protection against triptolide-induced toxicity in rat kidney cells, Toxicol. Lett. 213 (2) (2012) 194–202.
[13] I. Rudan, S. Sidhu, A. Papana, S.J. Meng, Y. Xin-Wei, W. Wang, R.M. Campbell-Page, A.R. Demaio, H. Nair, D. Sridhar, E. Theodoratou, B. Dowman, D. Adeloye, A. Majeed, J. Car, H. Campbell, W. Wang, K.Y. Chan, G Global Health Epidemiology Reference, Prevalence of rheumatoid arthritis in low- and middle-income countries: a systematic review and analysis, J Glob Health 5 (1) (2015) 010409.
[14] J.Z. Lin, J.J. Liang, J.D. Ma, Q.H. Li, Y.Q. Mo, W.M. Cheng, X.L. He, N. Li, M.H. Cao, D. Xu, L. Dai, Myopenia is associated with joint damage in rheumatoid arthritis: a cross-sectional study, J. Cach. Sarcop. Musc. 10 (2) (2019) 355–367.
[15] Y.J. Su, Y. Zhang, M. Chen, Z.Z. Jiang, L.X. Sun, T. Wang, L.Y. Zhang, Lipopolysaccharide exposure augments isoniazide-induced liver injury, J. Appl. Toxicol. 34 (12) (2014) 1436–1442.
[16] M.F.P. Ramos, A. Monteiro de Barros, C.V. Razvickas, F.T. Borges, N. Schor, Xanthine oxidase inhibitors and sepsis, Int. J. Immunopathol. Pharmacol. 32 (2018) 2058738418772210.
[17] Z.Q. Yuan, H.R. Zhang, M. Hasnat, J.X. Ding, X. Chen, P.S. Liang, L.X. Sun, L.Y. Zhang, Z.Z. Jiang, A new perspective of triptolide-associated hepatotoxicity: liver hypersensitivity upon LPS stimulation, Toxicology 414 (2019) 45–56.
[18] R.R. Hukkanen, W.G. Halpern, J.D. Vidal, Regulatory forum opinion piece: review of FDA draft guidance testicular toxicity-evaluation during drug development guidance for industry, Toxicol. Pathol. 44 (7) (2016) 927–930.
[19] FDA. U.S. FDA Guidance for Industry (Draft): Drug Interaction Studies – Study Design, Data Analysis, Implications for Dosing, and Labeling Recommendations [A/OL]. http://www.fda.gov/Drugs/GuidanceComplianceRegulatoryInformation/Guidances/ucm064982.htm (accessed 09 March 2017).
[20] Y. Nozaki, H. Kusuhara, T. Kondo, M. Hasegawa, Y. Shiroyanagi, H. Nakazawa, T. Okano, Y. Sugiyama, Characterization of the uptake of organic anion transporter (OAT) 1 and OAT3 substrates by human kidney slices, J. Pharmacol. Exp. Ther. 321 (1) (2007) 362–369.
[21] B. Feng, M.V. Varma, Evaluation and quantitative prediction of renal transporter-mediated drug-drug interactions, J. Clin. Pharmacol. 56 (Suppl 7) (2016) S110–S121.
[22] H.P. Wang, P.Y. Sun, C.Y. Wang, Q. Meng, Z.H. Liu, X.K. Huo, H.J. Sun, X.D. Ma, J.Y. Peng, K.X. Liu, Pharmacokinetic changes of cefdinir and cefditoren and its molecular mechanisms in acute kidney injury in rats, J. Pharm. Pharmacol. 70 (11) (2018) 1503–1512.
[23] S.L. Yang, Y.G. Dai, Z.H. Liu, C.Y. Wang, Q. Meng, X.K. Huo, H.J. Sun, X.D. Ma, J.Y. Peng, K.X. Liu, Involvement of organic cation transporter 2 in the metformin-associated increased lactate levels caused by contrast-induced nephropathy, Biomed. Pharmacother. 106 (2018) 1760–1766.
[24] M. Le Vee, V. Lecureur, B. Stieger, O. Fardel, Regulation of drug transporter expression in human hepatocytes exposed to the proinflammatory cytokines tumor necrosis factor-alpha or interleukin-6, Drug. Metab. Dispos. 37 (3) (2009) 685–693.
[25] W.A. Abualsunun, M. Piquette-Miller, STAT3 is involved in IL-6-mediated down-regulation of hepatic transporters in mice, J. Pharm. Pharm. Sci. 21 (1s) (2018) 325s–334s.
[26] M. Le Vee, E. Jouan, B. Stieger, V. Lecureur, O. Fardel, Regulation of drug transporter expression by oncostatin M in human hepatocytes, Biochem. Pharmacol. 82 (3) (2011) 304–311.
[27] W.N. Sun, Y.H. Ge, L.K. Yang, Y.P. Liu, X.Z. Liu, LC-MS quantification of triptolide and its transport across the caco-2 cell monolayer, Pharmaceut. Clin. Res. 24 (01) (2016) 15–18.
[28] Y.Y. Miao, L. Luo, T. Shu, H. Wang, Z.Z. Jiang, L.Y. Zhang, Study on difference of liver toxicity and its molecular mechanisms caused by Tripterygium wilfordii multiglycoside and equivalent amount of triptolide in rats, Chin. J. Chin. Mater. Med. (2019) 1–14.
[29] L.L. Kong, X.M. Zhuang, H.Y. Yang, M. Yuan, L. Xu, H. Li, Inhibition of P-glycoprotein gene expression and function enhances triptolide-induced hepatotoxicity in mice, Sci. Rep. 5 (2015) 11747.
[30] A. Gul, B. Kunwar, M. Mazhar, S. Faizi, D. Ahmed, M.R. Shah, S.U. Simjee, Rutin and rutin-conjugated gold nanoparticles ameliorate collagen-induced arthritis in rats through inhibition of NF-kappaB and iNOS activation, Int. Immunopharmacol. 59 (2018) 310–317.
[31] C.S. Heluany, L.V.K. Kupa, M.N. Viana, C.M. Fernandes, E.L.V. Silveira, S.H.P. Farsky, In vivo exposure to hydroquinone during the early phase of collagen-induced arthritis aggravates the disease, Toxicology 408 (2018) 22–30.
[32] M. Le Vee, P. Gripon, B. Stieger, O. Fardel, Down-regulation of organic anion transporter expression in human hepatocytes exposed to the proinflammatory cytokine interleukin 1beta, Drug. Metab. Dispos. 36 (2) (2008) 217–222.

[33] D. Huang, C.Y. Wang, Y.J. Duan, Q. Meng, Z.H. Liu, X.K. Huo, H.J. Sun, X.D. Ma, K.X. Liu, Targeting Oct2 and P53: formononetin prevents cisplatin-induced acute kidney injury, Toxicol. Appl. Pharmacol. 326 (2017) 15–24.
[34] R. Shi, Y.Y. Yang, Z.Y. Xu, Y. Dai, M. Zheng, T.M. Wang, Y.Y. Li, Y.M. Ma, Renal vectorial transport of berberine mediated by organic cation transporter 2 (OCT2) and multidrug and toxin extrusion proteins 1 (MATE1) in rats, Biopharm. Drug Dispos. 39 (1) (2018) 47–58.
[35] S.J. Wen, C.Y. Wang, Y.J. Duan, X.K. Huo, Q. Meng, Z.H. Liu, S.L. Yang, Y.N. Zhu, H.J. Sun, X.D. Ma, S.Y. Yang, K.X. Liu, OAT1 and OAT3 also mediate the drug-drug interaction between piperacillin and tazobactam, Int. J. Pharm. 537 (1–2) (2018) 172–182.
[36] T. Tai, X. Huang, Y.W. Su, J.Z. Ji, Y.J. Su, Z.Z. Jiang, L.Y. Zhang, Glycyrrhizin accelerates the metabolism of triptolide through induction of CYP3A in rats, J. Ethnopharmacol. 152 (2) (2014) 358–363.
[37] T.T. Yang, H.F. Mei, D.Q. Xu, W. Zhou, X.Y. Zhu, L.X. Sun, X. Huang, X. Wang, T. Shu, J. Liu, J.X. Ding, H.M. Hassan, L.Y. Zhang, Z.Z. Jiang, Early indications of ANIT-induced cholestatic liver injury: Alteration of hepatocyte polarization and bile acid homeostasis, Food. Chem. Toxicol. 110 (2017) 1–12.
[38] K. Mitsuoka, Y. Shirasaka, A. Fukushi, M. Sato, T. Nakamura, T. Nakanishi, I. Tamai, Transport characteristics of L-citrulline in renal apical membrane of proximal tubular cells, Biopharm. Drug. Dispos. 30 (3) (2009) 126–137.
[39] D. Taubert, G. Grimberg, W. Stenzel, E. Schomig, Identification of the endogenous key substrates of the human organic cation transporter OCT2 and their implication in function of dopaminergic neurons, PLoS One 2 (4) (2007) e385.
[40] Y.X. Zheng, L. Sun, T. Jiang, D.Q. Zhang, D.Y. He, H. Nie, TNFalpha promotes Th17 cell differentiation through IL-6 and IL-1beta produced by monocytes in rheumatoid arthritis, J. Immunol. Res. 2014 (2014) 385352.
[41] J.Y. Lee, J.K. Choi, N.H. Jeong, J. Yoo, Y.S. Ha, B. Lee, H. Choi, P.H. Park, T.Y. Shin, T.K. Kwon, S.R. Lee, S. Lee, S.W. Lee, M.C. Rho, S.H. Kim, Anti-inflammatory effects of ursolic acid-3-acetate on human synovial fibroblasts and a murine model of rheumatoid arthritis, Int. Immunopharmacol. 49 (2017) 118–125.
[42] J.H. Horstrup, M. Gehrmann, B. Schneider, A. Ploger, P. Froese, T. Schirop, D. Kampf, U. Frei, R. Neumann, K.U. Eckardt, Elevation of serum and urine levels of TIMP-1 and tenascin in patients with renal disease, Nephrol. Dial. Transp. 17 (6) (2002) 1005–1013.
[43] K. Musial, D. Zwolinska, Novel indicators of fibrosis-related complications in children with chronic kidney disease, Clin. Chim. Acta. 430 (2014) 15–19.
[44] K. Zhu, T. Zheng, X.H. Chen, H.M. Wang, Bioinformatic analyses of renal ischaemia-reperfusion injury models: identification of key genes involved in the development of kidney disease, Kidney Blood Press. Res. 43 (6) (2018) 1898–1907.
[45] G. Cakirca, F.H. Turgut, Serum matrix metalloproteinase-9, tissue inhibitor of metalloproteinase-1 and matrix metalloproteinase-9/neutrophil gelatinase-associated lipocalin complex levels in patients with early-stage diabetic nephropathy, Iran. J. Kidney Dis. 12 (5) (2018) 299–304.
[46] B. Bienias, P. Sikora, Urinary metalloproteinases and tissue inhibitors of metalloproteinases as potential early biomarkers for renal fibrosis in children with nephrotic syndrome, Medicine (Baltimore) 97 (8) (2018) e9964.
[47] W.R. Xue, Z.J. Zhang, S. Zeng, Y. Xu, Q. Zhang, W. Wang, Y. Zhang, X.D. Zhang, X.P. Hu, Expression and clinical significance of tissue inhibitor of metalloproteinases-1 (TIMP-1) and a disintegrin and metalloproteinase with thrombospondin type 1 motif 1 (ADAMTS1) in post-kidney-transplant bladder tumors, Ann. Transp. 22 (2017) 622–630.
[48] S.J. Sohn, S.Y. Kim, H.S. Kim, Y.J. Chun, S.Y. Han, S.H. Kim, A. Moon, *In vitro* evaluation of biomarkers for cisplatin-induced nephrotoxicity using HK-2 human kidney epithelial cells, Toxicol. Lett. 217 (3) (2013) 235–242.
[49] X. Qiu, X.B. Zhou, Y.F. Miao, B. Li, An in vitro method for nephrotoxicity evaluation using HK-2 human kidney epithelial cells combined with biomarkers of nephrotoxicity, Toxicol. Res. (Camb) 7 (6) (2018) 1205–1213.
[50] L.L. Peng, J.Y. Yang, C. Ning, J. Zhang, X.C. Xiao, D. He, X.Y. Wang, Z.P. Li, S.S. Fu, J.P. Ning, Rhein inhibits integrin-linked kinase expression and regulates matrix metalloproteinase-9/tissue inhibitor of metalloproteinase-1 ratio in high glucose-induced epithelial-mesenchymal transition of renal tubular cell, Biol. Pharm. Bull. 35 (10) (2012) 1676–1685.
[51] R.F. van Vollenhoven, Sex differences in rheumatoid arthritis: more than meets the eye, BMC Med. 7 (2009) 12.
[52] H.P. Song, X. Li, R. Yu, G. Zeng, Z.Y. Yuan, W. Wang, H.Y. Huang, X. Cai, Phenotypic characterization of type II collagen-induced arthritis in Wistar rats, Exp. Ther. Med. 10 (4) (2015) 1483–1488.
[53] Z.Z. Jiang, X. Huang, S. Huang, H.L. Guo, L. Wang, X.J.Y. Li, X. Huang, T. Wang, L.Y. Zhang, L.X. Sun, Sex-related differences of lipid metabolism induced by triptolide: the possible role of the LXRalpha/SREBP-1 signaling pathway, Front. Pharmacol. 7 (2016) 87.
[54] I. Sabolic, A.R. Asif, W.E. Budach, C. Wanke, A. Bahn, G. Burckhardt, Gender differences in kidney function, Pflugers Arch. 455 (3) (2007) 397–429.
[55] A. Gandhi, B. Moorthy, R. Ghose, Drug disposition in pathophysiological conditions, Curr. Drug. Metab. 13 (9) (2012) 1327–1344.
[56] M. Xue, Y. Zhao, X.J. Li, Z.Z. Jiang, L. Zhang, S.H. Liu, X.M. Li, L.Y. Zhang, S.Y. Yang, Comparison of toxicokinetic and tissue distribution of triptolide-loaded solid lipid nanoparticles vs free triptolide in rats, Eur. J. Pharm. Sci. 47 (4) (2012) 713–717.
[57] J.R. Lin, B. Lin, H.T. Song, Research progress on in vivo pharmacokinetics of triptolide and celastrol, Chin. Trad. Herb. Drugs. 47 (3) (2016) 528–532.
[58] J.Q. Liu, Q. Li, R. Zhang, F. Liu, W. Zhang, Z.H. He, Q. Hong, X.L. Kou, J.M. Wu, LC-MS/MS studies on effect of *Glycyrrhiza uralensis* on metabolism distribution and excretion of triptolide in rat, Chin. J. Pharm. Anal. 16 (9) (2010) 151–156.
[59] Z.D. Tan, R. Zhu, R. Shi, J. Zhong, Y.M. Ma, C.H. Wang, X.H. Wang, N.N. Cheng, Involvement of rat organic cation transporter 2 in the renal uptake of jatrorrhizine, J. Pharm. Sci. 102 (4) (2013) 1333–1342.
[60] H. Motohashi, K. Inui, Organic cation transporter OCTs (SLC22) and MATEs (SLC47) in the human kidney, AAPS J 15 (2) (2013) 581–588.
[61] H.J. Burt, S. Neuhoff, L. Almond, L. Gaohua, M.D. Harwood, M. Jamei, A. Rostami-Hodjegan, G.T. Tucker, K. Rowland-Yeo, Metformin and cimetidine: physiologically based pharmacokinetic modelling to investigate transporter mediated drug-drug interactions, Eur. J. Pharm. Sci. 88 (2016) 70–82.
[62] L.P. Li, F.F. Song, Y.Y. Weng, X. Yang, K. Wang, H.M. Lei, J. Ma, H. Zhou, H.D. Jiang, Role of OCT2 and MATE1 in renal disposition and toxicity of nitidine chloride, Br. J. Pharmacol. 173 (16) (2016) 2543–11554.
[63] Y. Lu, T. Xie, Y.J. Zhang, F.Q. Zhou, J. Ruan, W.N. Zhu, H.X. Zhu, Z. Feng, X.P. Zhou, Triptolide Induces hepatotoxicity via inhibition of CYP450s in Rat liver microsomes, BMC Compl. Altern. Med. 17 (1) (2017) 15.
[64] Y. Wang, A.H. Moser, J.K. Shigenaga, C. Grunfeld, K.R. Feingold, Downregulation of liver X receptor-alpha in mouse kidney and HK-2 proximal tubular cells by LPS and cytokines, J. Lipid. Res. 46 (11) (2005) 2377–2387.
[65] T. Wongwan, S. Kittayaruksakul, N. Asavapanumas, V. Chatsudthipong, S. Soodvilai, Activation of liver X receptor inhibits OCT2-mediated organic cation transport in renal proximal tubular cells, Pflugers Arch. 469 (11) (2017) 1471–1481.